Accepted Manuscript

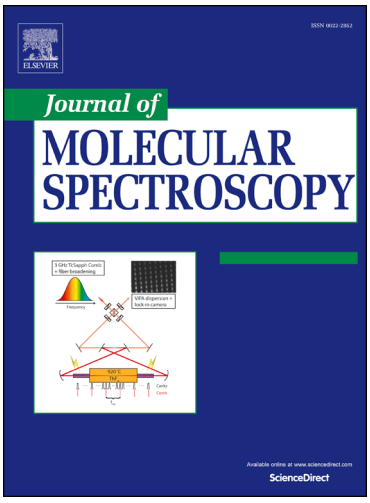

Vibrationally-Resolved Photoelectron Spectroscopy and Photoelectron Circular Dichroism of Bicyclic Monoterpene Enantiomers

Hassan Ganjitabar, Rim Hadidi, Gustavo A. Garcia, Laurent Nahon, Ivan Powis

PII: S0022-2852(18)30175-9
DOI: https://doi.org/10.1016/j.jms.2018.08.007
Reference: YJMSP 11074

To appear in: *Journal of Molecular Spectroscopy*

Received Date: 14 May 2018
Revised Date: 11 July 2018
Accepted Date: 22 August 2018

Please cite this article as: H. Ganjitabar, R. Hadidi, G.A. Garcia, L. Nahon, I. Powis, Vibrationally-Resolved Photoelectron Spectroscopy and Photoelectron Circular Dichroism of Bicyclic Monoterpene Enantiomers, *Journal of Molecular Spectroscopy* (2018), doi: https://doi.org/10.1016/j.jms.2018.08.007

Version 11 July 2018

Vibrationally-Resolved Photoelectron Spectroscopy and Photoelectron Circular Dichroism of Bicyclic Monoterpene Enantiomers

Hassan Ganjitabar[1], Rim Hadidi[2], Gustavo A. Garcia[2], Laurent Nahon[2], and Ivan Powis[1,]*

[1] School of Chemistry, The University of Nottingham, University Park, Nottingham NG7 2RD, UK.

[2] Synchrotron SOLEIL, l'Orme des Merisiers, Saint Aubin BP 48, 91192 Gif sur Yvette Cedex, France.

*Corresponding Author:
Tel: +44 115 9513467
E-mail: ivan.powis@nottingham.ac.uk

Abstract

The photoionization of four chiral bicyclic monoterpene isomers, α-pinene, β-pinene, 3-carene and sabinene — all commonly found constituents in essential natural oils — has been studied using synchrotron radiation and compared to recent findings for the cyclic isomer limonene. Slow photoelectron spectra (SPES) are recorded between threshold and an energy of 10.5 eV. In the case of limonene, α-pinene, and 3-carene, vibrational structure is observed in the ground ionic state and attributed to a C=C double bond stretching in the cation, using Franck-Condon vibrational band simulations. The photoelectron circular dichroism (PECD) is examined for specific enantiomers of these terpenes, and vibrational modification of the forward-backward photoelectron asymmetry detected by PECD can be tentatively identified, even when the corresponding SPES is unstructured. Large chiral asymmetry factors are found at low binding energies for the pinenes and 3-carene, with α-pinene in particular displaying a 37% forward-backward photoelectron asymmetry, believed to be a record chiroptical asymmetry for randomly-oriented, non-interacting molecules.

Introduction

The monoterpene family of $C_{10}H_{16}$ isomers significantly contributes to the annual loading of biogenic volatile organic compounds (BVOC) emissions. Consequently, the potential role of terpenes in atmospheric chemistry, for example the formation of secondary organic aerosols (SOA) with human health implications, has long been recognised. Monoterpenes such as limonene and the pinenes have distinctive odours and nowadays are extensively used commercially in scents, toiletries, cosmetics, domestic cleaning agents and air fresheners, and in consequence these have also been identified as among the most prevalent VOCs in modern urban and domestic environments.[1] Recently, even domestic cooking activities have been considered as generators of indoor monoterpene concentrations.[2]

Many of the monoterpene isomers are chiral, and in recent decades there has been a growing awareness and interest in their enantiomer specific properties. Monoterpenes are ubiquitous in essential oil extracts where, as volatile odorants, they greatly contribute to the aromas. A sometimes subtle factor underpinning this is that many monoterpene enantiomer pairs in fact have distinctly different perceived odours.[3] The enantiomer composition of monoterpene BVOC emissions has been studied in field studies of environments such as plantations, forests,[4-6] and even the marine environment.[7] Variations in enantiomeric ratios are found between species and geographical location, but also in response to conditions such as plant stress. This indicates that chiral analysis may become an important diagnostic probe in an era of rapid climate change. Moreover, the natural variation in enantiomer ratios with growing season and location suggests that enantiomeric analysis may play an important role in formulation, authentication and traceability of, for example, citrus fruit extracts[8,9] or teas.[10]

A recent proof of principle paper[11] demonstrated how the technique of mass-selected photoelectron circular dichroism (MS-PECD) could be exploited to provide simultaneous enantioselective detection and identification of prepared chiral molecule vapours containing limonene (a cyclic monoterpene) and camphor. In preparation for more ambitious applications of MS-PECD to decipher chemical and enantiomeric composition of essential oil extracts, we were motivated to study here a greater number of monoterpene enantiomer samples to be used a database of elementary compounds. PECD techniques permit enantiomeric excess (e.e.) to be determined to better than 1% [12-14], comparable to the best chromatographic methods, so that this approach appears to have real potential for the kinds of application outlined above.

Photoelectron circular dichroism[15,16] measures a forward-backward asymmetry in the angular emission of photoelectrons upon ionization of a chiral molecule with circularly polarized light. These asymmetries typically range from a few- to a few tens percent, and so are orders of magnitude greater than other molecular chiroptical asymmetry measurements. The sensitivity this confers allows the direct application of PECD to dilute organic vapours. As arguably the most important terpene, limonene has been studied with both short pulse laser multiphoton ionization (MP-)PECD methods[11,17-19] and by single photon ionization using synchrotron radiation.[20] A theme that emerges from these investigations concerns the role of vibrational excitation. The photoelectron spectrum of limonene displays pronounced vibrational structure, and the PECD asymmetry evidently is modulated by the degree of vibrational excitation in the ionization process. This had previously been observed in small chiral oxiranes and predicted in ideal systems,[21] sometimes as a complete reversal of the forward-backward asymmetry on excitation of weak vibrational modes[22,23], but finding a similar phenomenon in a larger $C_{10}H_{16}$ species was nevertheless unexpected.[20] Taking this forward to develop a full understanding in the case of limonene one encounters two difficulties: (i) an uncertain

conformer population; (ii) close lying HOMO and HOMO-1 electrons whose ionization overlaps in the first photoelectron band.

In the present work we examine four more monoterpenes, α-pinene, β-pinene, 3-carene, and sabinene using synchrotron radiation (see Fig. 1). Unlike limonene, the more rigid bicyclic structure of these choices restricts the feasible geometry to a single conformation, and a greater energetic separation of the first two orbitals eliminates the uncertainty of overlapping ionizations. For each of these four species the photoelectron spectroscopy is first examined to identify, where possible, the nature of any vibrational excitation. Secondly the PECD associated with the HOMO ionization is measured and reported. In the case of α-pinene this has allowed us to record what we believe is the largest chiroptical asymmetry, 37%, to have been observed in non-interacting (i.e. discounting excitonic chiral amplification) randomly-oriented chiral molecules to date. Some limonene data has also been re-measured, but under conditions that are standardised for all samples in order to provide a consistent database for future analytical applications. It is also with these applications in mind that we provide the fragmentation pattern for the five terpenes, including limonene, as Supplementary Information, which can be used for species identification, especially in synchrotron-based mass spectrometry experiments.[24] For convenience in comparing limonene with the four additional terpenes in this study, relevant conclusions drawn from a previous study of limonene [20] are briefly summarised in the discussion developed here.

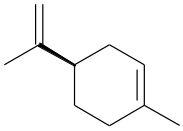

R-(+)-limonene

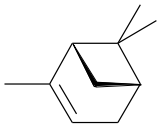

(1R,5R)-(+)-α-pinene

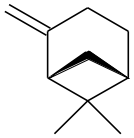

(1S,5S)-(-)-β-pinene

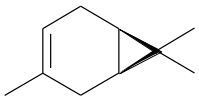

1S-(+)-3-carene

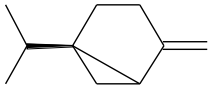

(1S,5S)-(-)-sabinene

Figure 1

Experimental

Measurements were made using the DELICIOUS 3 double imaging (i^{2}PEPICO) spectrometer,[25] equipping the permanent molecular beam end-station SAPHIRS[26] on the undulator-based variable-polarization DESIRS vacuum ultraviolet (VUV) beamline[27] at Synchrotron SOLEIL. This provides velocity map imaging (VMI) of the electrons, and simultaneously ion 3D momentum determination of coincident ions. It is thus possible to tag the electron data with the mass and kinetic energy of the corresponding cation formed.

For all the samples presented in this work, two types of experiment were performed: threshold photoelectron spectroscopy and fixed photon energy PECD. Both types of measurement were

performed detecting the electrons in electron-ion coincidence mode, allowing the electron spectra and angular distributions to be mass-tagged with the coincident ion mass when desired. The photoelectron spectra were first obtained by scanning the photon energy and recording the signal of threshold electrons applying the slow photoelectron spectroscopy technique or SPES.[28,29] Briefly, the photoelectron signal $\mathrm{I}(h\nu, eKE)$is recorded as a function of photon and electron kinetic energy. Threshold photoelectron spectra (TPES) only take into account threshold electrons with the resolution being roughly equal to the maximum electron signal integration eKE_{max}: $\mathrm{TPES}(h\nu) = \int_0^{eKE_{max}} I(h\nu, eKE)deKE$. As previously reported, the SPES method offers a better compromise between signal and resolution by taking advantage of the energy conservation to increase the electron bandwidth by integrating along the diagonal lines of unity slope $\mathrm{eKE} = \mathrm{h}\nu - IE_i$, where IE_i represents the ionization energy of the *i*th state. The SPES spectra are then given by the expression: $\mathrm{SPES}(h\nu) = \int_0^{eKE_{max}} I(h\nu + eKE, eKE)deKE$. For instance, in the present experiments, the electron bandwidth was chosen as eKE_{max}=70 meV, but contrary to the TPES, the corresponding resolution is much better, at 15 meV. The photon energy was scanned between 7.8 and 10.5 eV with 5 meV steps and the monochromator was set to provide energy resolutions in the 4 to 6 meV range. A gas filter filled with Kr ensured spectral purity by cutting off the higher harmonics from the undulator,[30] while the observation of a Kr absorption line during wavelength scans provided an independent wavelength calibration check. State selected ion fragmentation curves were extracted from the same photon energy scans, as described and presented in Supplementary Information.

PECD occurs as an asymmetry in the photoelectron angular distribution. Phenomenologically, for a single photon ionization (but allowing for the possibility of ionization of a chiral species with circularly polarized light) this normalised distribution can be written as

$$\mathrm{I_p}(\theta) = 1 + \mathrm{b_1^{(p)}P_1}(\cos\theta) + \mathrm{b_2^{(p)}P_2}(\cos\theta),$$

where $\mathrm{p} = \pm 1$ is an index for respectively left- and right- circular polarization, θ is the emission direction relative to the photon beam, and $\mathrm{P_j}$ are the first and second order Legendre polynomials. The angular distribution parameters $\mathrm{b_j^{(\pm 1)}}$ obey certain symmetry rules, but notably $\mathrm{b_1^{(+1)}} = -\mathrm{b_1^{(-1)}}$ and is necessarily zero for achiral molecules. Hence the chiral asymmetry is defined by the $\mathrm{b_1^{(p)}}$ parameter and the maximum asymmetry factor $\mathrm{g} = \mathrm{I_{+1}}(\theta) - \mathrm{I_{-1}}(\theta)$ can be shown to be simply $2\mathrm{b_1^{(+1)}}$ at $\theta = 0°, 180°$.

The mass-selected PECD (PECD-PICO)[31] was obtained for a given photon energy by recording mass-selected photoelectron images and alternating the light helicity (left/right circularly polarized light: LCP/RCP) every 15 minutes. As previously reported,[32] after summing up all the contributions into a pair of LCP and RCP images, the photoelectron spectrum is extracted after Abel inversion of the total image (LCP+RCP), while the PECD is obtained from inversion of the difference image (LCP-RCP). Note that the data have not been corrected by the degree of circular polarization due to the high purity in the undulator emission polarization, S_3>=0.97, where S_3 is the Stokes parameter measuring the absolute degree of circular polarization.

Identical conditions were used for the series of measurements on all isomers. The liquid sample was contained at room temperature in a bubbler through which He gas was flowed at 0.5 bar pressure. The He/vapour mix was then allowed to expand into vacuum through a 70 μm nozzle to form a seeded molecular beam. This was passed via a double skimmer arrangement into the spectrometer chamber, where it was intersected in the DELICIOUS3 source region by the synchrotron beam.

Enantiomeric samples of (+)-1R,5R-α-pinene, (-)-1S,5S-β-pinene, (+)-1S,6R-3-carene, and (+)-4R-limonene were obtained from Sigma-Aldrich and used without further purification. The limonene and α-pinene were specified to have >97 % enantiomeric excess. The e.e. for the β-pinene and 3-carene samples was not specified, but we commissioned a two-column gas chromatography (GC^2) chiral analysis of our samples that confirmed the above e.e. values as stated and found the $e.e._S$ of β-pinene was 94%, and that of 3-carene was ≥99%.

Pure sabinene samples were not commercially available, even as a racemic sample, so we obtained a natural extract of sabinene of stated purity ≥75% (Sigma-Aldrich). The GC^2 analysis of this sample found the sabinene content to be 75.94 ± 0.46 % with the remainder being β-pinene. Interestingly, the $e.e._S$ of the sabinene was found to be 86.69 ± 0.47 % while that of the β-pinene component was 80.34% ± 0.53 %. We can use these values to estimate corrections for the photoelectron spectrum and circular dichroism measured for the sabinene extract, as described in the Supplementary Information (SI).

Computational

Geometry optimisation and harmonic frequency calculations for both neutrals and ground state cations were performed at the MP2/6-31G** and B3LYP/cc-pVTZ levels using Gaussian09.[33] These resulted in very similar Franck-Condon (FC) simulations of the photoelectron, but the MP2 results former were deemed to be slightly preferable and so are those reported here. The vertical ionization energies were calculated at the MP2/6-31G** neutral geometries using the outer valence Green's function (OVFG) method implemented in Gaussian 09 with a cc-pVTZ basis.

The FC simulations were performed using the FCLab-II package.[34] Unless otherwise stated harmonic frequencies were scaled by a factor 0.97 before use, and only the vibrationless state of the neutral molecule was considered, meaning that any hot band structure is overlooked. Once a stick spectrum has been obtained it is convoluted with a shaping function to achieve a more realistic looking simulation. In doing this we have not, however, attempted to match exactly the widths of any experimental peaks. The FC simulation evaluates the energies of all vibrational transitions relative to the 0-0 origin, and hence don't directly incorporate the electronic excitation energy. In preparing comparison plots an energy offset is applied to the simulation plots, the value of which can then be interpreted as representing the adiabatic 0-0 ionization energy.

Results

Photoelectron Spectra

Limonene

We commence the presentation of the photoelectron spectra with limonene. In fact the VUV photoionization of limonene has been extensively studied and reported in a recent paper,[20] but in this section it is convenient to replot the SPES and simulation from that work as Fig. 2. We briefly summarise the previous findings here to facilitate a subsequent discussion and comparison ranging across the other newly examined monoterpene isomers.

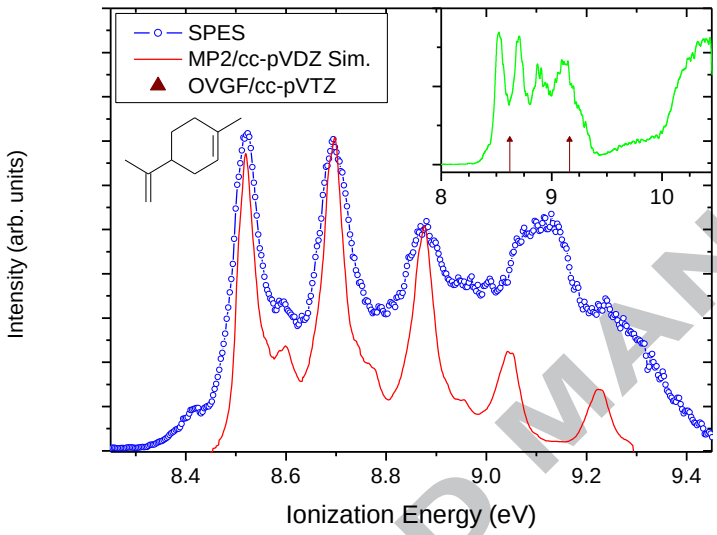

Figure 2

Limonene has two close-lying outer π orbitals. The 2π HOMO is located at the endo-cyclic double bond in the 6 membered ring and the 1π (HOMO-1) at the exo-cyclic C=C bond in the isopropenyl tail. As confirmed by the OVGF calculated vertical ionization energies (inset of Fig. 2), the higher energy region of the first SPES band (≥ 8.85 eV) most likely spans both of these orbital ionizations. The band still, however, has strong vibrational features and a FC simulation provides a good reproduction of these, at least on the low energy side of the band, below the likely onset of the $1\pi^{-1}$ ionization. The features are thus assigned as a pseudo progression in excited quanta of the ring C=C stretching mode, albeit with many other associated, poorly resolved combination transitions.

Various conformer structures of limonene have been identified, the three most stable of which have the isopropenyl tail group in an equatorial position. In a cooled jet expansion it was deduced that the least stable conformer is effectively frozen out, leaving just two conformations which probably are in approximately equal population. The vibrational simulations for these two conformations are almost indistinguishable, so offer no means to distinguish relative contributions.

The adiabatic ionization energy was determined as 8.505 eV, with the vertical ionization peak at 8.524 eV,[20] the latter in excellent agreement with a previous high resolution He I PES.[35]

The dissociative ionization data showing the production (total and state-selected) of different fragment cations is shown in Figure S5 of the SI.

α-pinene

The bicyclic ring structure of α-pinene suggests it should be rigid. A recent supersonic molecular beam Fourier Transform Microwave (FTMW) spectroscopy investigation[36] has indeed shown α-pinene to possess just a single conformer having a quasi-planar structure for its 6 membered ring. This was confirmed at the time with B3LYP/6-311++G(2df,p) and MP2 calculations, the latter using an aug-cc-pVTZ basis set with added polarization functions. We have subsequently achieved the same result using MP2/6-31G** calculations whilst also performing a harmonic vibrational analysis for a subsequent Franck-Condon simulation.

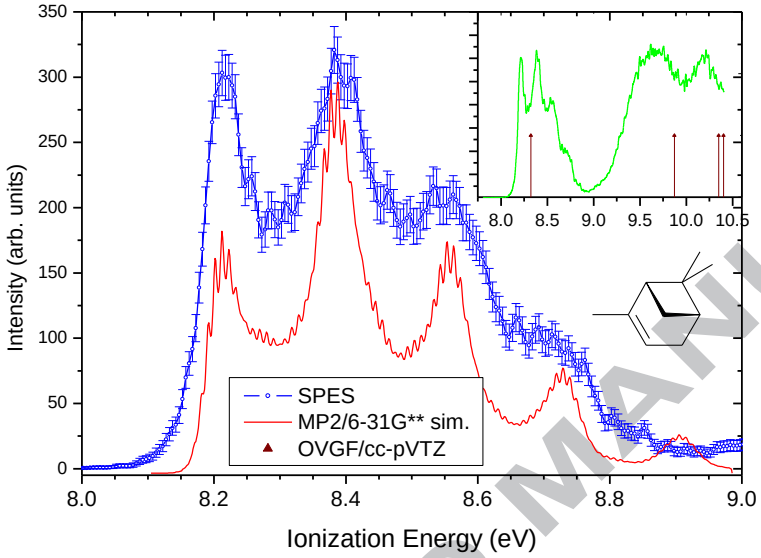

Figure 3

Fig. 3 shows the experimental SPES recorded for α-pinene. The first band possesses a strong vibronic structure, somewhat similar to limonene. Unlike limonene, where the HOMO and HOMO-1 ionizations overlap, this band can be uniquely assigned as ionization of the HOMO which can be characterised as the CC double bond localised π orbital. The next deeper orbitals are well separated in energy, and so give rise to separate photoelectron bands, as confirmed by the OVGF/cc-pVTZ calculations for vertical ionization energies (inset Fig. 3). Note that the corresponding electronically excited cation states are not stable, and fragment to daughter ions, as seen in the mass-selected SPES shown in Figure S3 of the SI.

The first two prominent peaks observed in the HOMO band are measured at 8.21 eV and 8.38 eV, the second seeming in excellent agreement with the vertical ionization energy of 8.38 eV previously reported, albeit from a much lower resolution He I PES measurement.[37] Fig. 3 includes the results of our Franck-Condon simulation, for which the MP2/6-31G** vibrational frequencies have been scaled by a factor 0.89. The stick spectrum of transition energies/intensities has been convoluted with an arbitrarily chosen shaping function to generate a more realistic appearance, although exact reproduction of the experimental widths has not been attempted. The overall appearance of the simulation is a very good match with the experiment, and by aligning the two and then noting the position of the 0-0 origin transition on the experimental scale we can further estimate the adiabatic ionization energy to be 8.16 eV. This is a little lower than the 8.3 ± 0.02 determined by Kubala et al[38] from ion yield curves, but these authors were using electron impact ionization and fitting to locate the buried adiabatic threshold.

The experimental separation of the prominent features in the first photoelectron band, ~0.17 eV (≈1370 cm^{-1}), is very similar to that noted in limonene. From the simulation it is possible to identify the features as a pseudo-progression in excitations of the C=C double bond stretching mode, ν_{56}^{+}, with a calculated harmonic frequency of 1412 cm^{-1} (scaled); this simple C=C stretching motion, however, occurs in combinations with many other low frequency deformation modes.

3-carene

The bicyclic ring structure of 3-carene again suggests a rigid structural form, but for a long time the precise conformation was uncertain, with various experimental interpretations and theoretical calculations disagreeing on whether it adopted a chair or boat conformation. More recent, high level calculations[39] (CCSD/aug-cc-pVDZ, B3LYP/aug-cc-pVTZ) have found 3-carene to possess a single stable conformer with a near planar six-membered ring. This article also provides a nice summary of the earlier evidence and ensuing controversies.

The SPES recorded for 3-carene is shown in Fig. 4 along with a Franck-Condon vibrational simulated

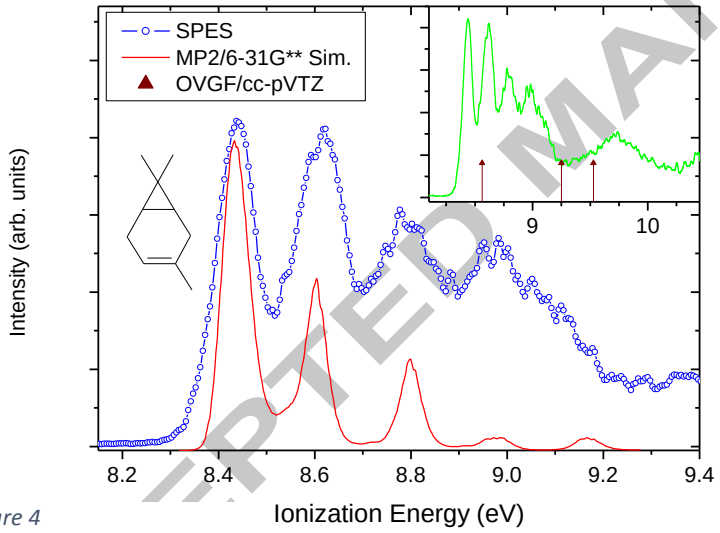

Figure 4

spectrum for the HOMO ionization band. This outermost orbital is predicted to be a π orbital located on the C=C double bond. The OVGF vertical ionization energies allow this first band to be associated predominantly with the π^{-1} ionization, but the next two ionization energies fall lower than the obvious next band in the experimental spectrum (inset, Fig. 4). There is thus some uncertainty about these deeper lying ionizations. As seen in Figure S4 and Table S1 of the SI, the fragmentation onset is at 9.05 eV, which is close to the calculated vertical ionization energy for the HOMO-1, implying that it is this second electronic state of the ion that is dissociative.

The FC simulation using MP2/6-31G** calculated harmonic frequencies is shown in the figure. By aligning the simulation with the experimental spectrum, the 0-0 origin can be estimated to lie at 8.38 eV. This compares well with a previously reported adiabatic I.E. of 8.4 eV (I_{vert}= 8.61 eV) obtained by photoelectron spectroscopy.[40]

There is again a strong vibrational structure evident in the experimental spectrum, with a principal peak separation of ~0.185 eV (≈1490 cm^{-1}), a little greater than that noted for limonene and α-pinene. The FC simulation allows us to identify the structure as pseudo-progression of successive

quanta in the C=C double bond stretching mode, υ_{56}^{+} = 1569 cm^{-1} (scaled) appearing in combinations with many other low frequency deformation modes. These additional, unresolved, transitions cause an asymmetric broadening of the observed peaks with a consequent displacement of the observed positions of the maxima.

β-pinene

β-pinene has a bicyclic structure that provide it also with a rigid, single conformation structure as confirmed by B3LYP/6-311+G* calculations[41] and more recent calculations using composite methods (G3MP2[38] and CBS-QB3[42]). Nevertheless, it possesses several low frequency vibrational modes that may be significant for determining its chiroptical properties.[43]

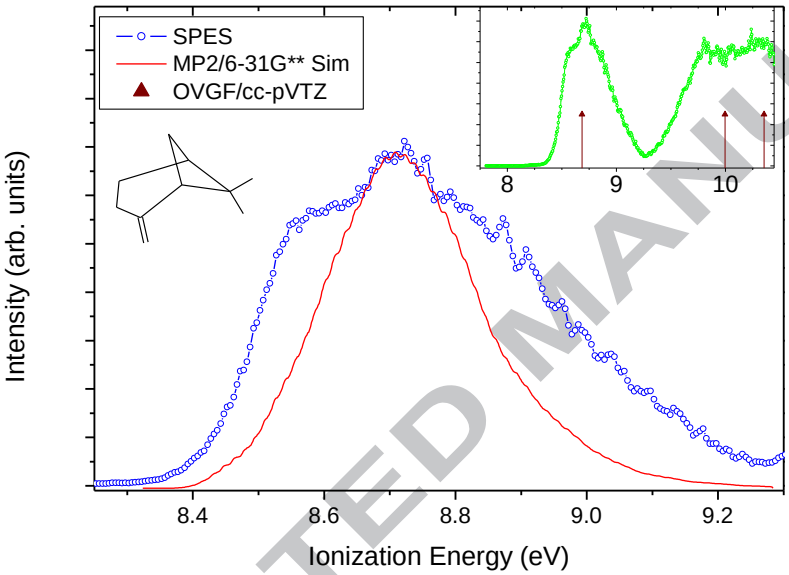

Figure 5

The HOMO in this isomer is again a π bonding orbital localised at the C=C double bond but which, in this case is exo-cyclic. It is predicted to be energetically well separated from subsequent deeper valence orbitals, and this is reflected in the calculated OVGF ionization energies, which also correspond closely to the band structure in the experimental SPES. The inset to Fig. 5 shows this comparison of the OVGF/cc-pVTZ calculated vertical ionization energies and the outer valence region SPES of β-pinene. As seen in the state-selected dissociative ionization data presented in Figure S6 of the SI, only ionization from the HOMO orbital leaves the ion intact , while ionization of inner orbitals produces exclusively unstable ions.

Photoion yield measurements have previously determined an adiabatic ionization energy of 8.45 ± 0.03 eV, compared with their calculated value of 8.38 eV. [42] The latter looks in close agreement with our current threshold behaviour.

The HOMO band SPES (Fig. 5) is relatively broad and lacking in vibrational structure compared to other terpenes (limonene, α-pinene, 3-carene), although there is a prominent shoulder observed to low energy of the peak maximum. While the MP2/6-31G** FC simulation shown in Fig. 5 confirms a lack of distinct vibrational structure, it provides poor agreement with experiment, with the overall

band width being too narrow. Having discounted multiple conformers and overlapping ionization bands, the HOMO peak envelope must be attributable to vibrational excitation, which the calculation evidently fails to reproduce. It can be noted that both the G3MP2 [38] and CBS-QB3 [42] geometry optimisations for the ground state cation conclude that the HOMO ionization induces a ring opening in the ionic state, and we find this to be replicated by our more modest B3LYP/cc-pVTZ, and an alternative B3LYP/6-311G** calculations.[1] As a consequence of the large geometry change indicated between neutral and ion, our B3LYP vibrational simulations fail, resulting in vanishingly small predicted FC factors. In contrast MP2 calculations suggest a bond extension (to ~1.78 A) rather than a full ring opening, allowing the MP2 based FC simulation some partial success (shown in Fig. 5); nevertheless it falls well short of fully reproducing the experimental results, and suggests a more ambitious approach is required to model vibrational excitation in this system.

Sabinene

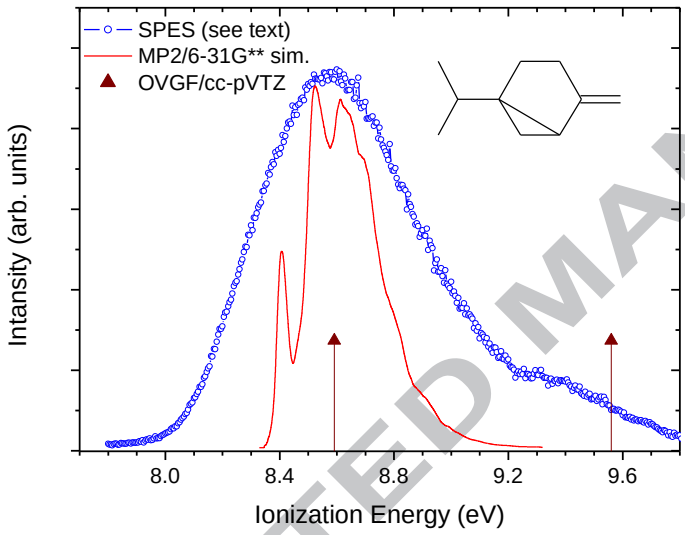

Figure 6

Sabinene has, again, a bicyclic structure suggesting a high degree of rigidity. Low resolution microwave spectroscopy was used to infer a boat like structure for the six-membered ring of sabinene,[44] but we are not aware of any subsequent work on this molecule. In our own calculations (B3LYP/cc-pVTZ, B3LYP/6-311G** and MP2/6-31G**) we found that the boat form was indeed the most stable, but also noted a stable chair-like geometry in the MP2 calculation. Since this was ~14.7 kJ mol^{-1} higher in energy we have, however, discounted any contribution in a room temperature or colder sample. Analogous to the β-pinene case, we also found that the B3LYP calculations, but not the MP2 calculation, predicted the strained three membered ring to open in the cation state.

Fig. 6 shows our estimated pure sabinene SPES, derived from a recording made with the impure natural extract. This spectrum was prepared by subtraction of the β-pinene SPES, appropriately weighted. Both impure sabinene and β-pinene spectra were recorded under identical experimental conditions (sample temperature, backing pressure, photon settings). A full description of the process followed to achieve an effective correction for the minor β-pinene component is provided in the Supplementary Information.

[1] The distance $r_{C\text{-}C}$ increases from 1.57 Å in the neutral to ~2.3 Å in the cation

The peak position of the derived sabinene SPES (8.58 eV) is in good agreement with the OVGF/cc-pVTZ calculated sabinene vertical ionization energy (8.59 eV) for the HOMO orbital, which can be characterised as predominantly a C=C π electron, as for the other isomers considered here. Ionization of HOMO-1 is predicted to require nearly 1 eV more energy, so that the photoelectron band shown in Fig 6 can be confidently assigned as the single ionization of the HOMO orbital alone. Ionization of orbitals other than the HOMO leads to dissociation of the resulting parent cation, as shown in the state-selected dissociative ionization data presented in Figure S7 of the SI.

Also included in Fig 6 is the FC simulation of vibrational structure for the HOMO ionization. The plotting offset for this has been arbitrarily judged to best match the apparent vertical ionization energies, but the overall agreement with our experimental result is clearly poor, the simulated band having a much narrower width. While this theory-experiment plotting comparison positions the calculated 0-0 origin transition at an ionization energy of 8.39 eV, the onset of the experimental result suggests a true adiabatic ionization energy closer to 8 eV.

Photoelectron circular dichroism

For all our terpene molecules we have recorded VMI images for alternate left- and right-circular polarizations at photon energies of 9.0 and 9.5 eV, keeping all other sample conditions identical. This includes limonene for which, despite an earlier, in-depth investigation[20], no strictly comparable measurement at 9 eV was previously available. The left-and right-images are then processed as previously described to extract a PES and PECD, the latter in the form of the normalised chiral angular distribution parameter, $b_1^{(+1)}$. In the data presented below (VMI PES and PECD) the electrons have been filtered by mass-tagging with the coincident parent ion mass (m/z 136). This discriminates against any background from scattered electrons from higher energy, dissociative cation states, which in the cases discussed here perfectly discriminates against all orbitals other than the HOMO, as can be inferred from the dissociative behaviour discussed in Supplementary Information. Limonene is the one exception since both its HOMO and HOMO-1 ionizations are non-

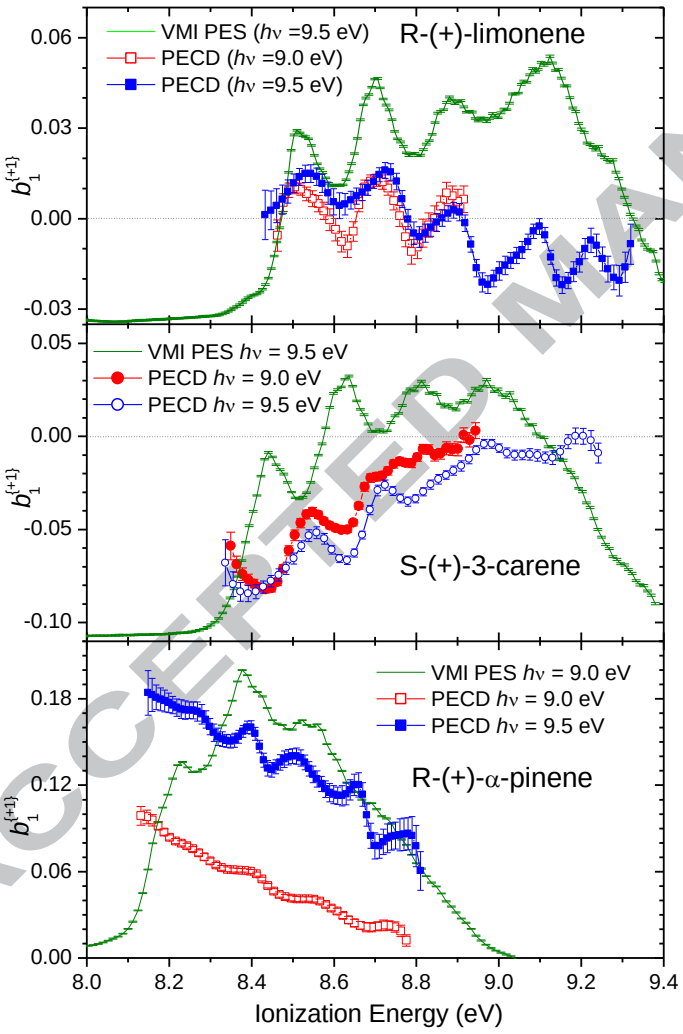

Figure 7

dissociative. This also corresponds to potential analytical applications where m/z 136 mass-tagged PECD may be used to identify monoterpene components in mixtures.[11]

In Fig. 7 we show these measurements for R-(+)-limonene, S-(+)-3-carene, and R-(+)-α-pinene. In the same figure we include the *h*ν = 9.5 eV VMI PES, plotted on the same energy scale, for convenient

comparison. The energy resolution of these VMI PES (and PECD) measurements will be somewhat less than the SPES measurements made by scanning through threshold electron yields as shown in the preceding section. The very different PECD of these three isomers will be immediately obvious from a visual examination of the figure.

The general form and characteristics of the limonene PECD in this relatively low photon energy region have been discussed previously.[20] Again, for convenience we summarise those findings here. Most strikingly, the limonene PECD modulates with the principal vibrational features observed in the PES, even switching sign between the peaks and valleys in the measurement made at 9 eV photon energy. This means that the preferred direction of the forward-backward asymmetry in the angular emission of electrons will flip, relative to the photon beam direction, in step with the vibrational excitation of the cation. However, a full interpretation of the limonene PECD is compromised by: (a) the onset of the second ionization channel, $1\pi^{-1}$ above 8.85 eV, where it then overlaps the HOMO $2\pi^{-1}$ channel; (b) the uncertain conformer population, since PECD is both orbital specific and can be extremely sensitive to conformation.[15,45-47] It is these uncertainties that motivate the present study of other terpene isomers.

The 3-carene measurements in Fig. 7 look superficially similar, in that the PECD is again quite strongly modulated with the principal vibrational peaks in the PES, and does not change greatly with this limited range of photon energies. On the other hand, the absolute magnitude of the recorded PECD for 3-carene is greater with a peak chiral asymmetry, $2\left|b_1^{(\pm1)}\right|$, of ~17 % (compared to ~5% for limonene)

The PECD measurements for α-pinene recorded at 9.5 eV photon energy once again apparently reflect the clear vibrational structure of the PES although the modulation (in both the VMI PES and PECD) is weaker than for limonene and 3-carene. In the hν = 9.0 eV PECD measurement only a very weak oscillation is seen. There is also a very large difference in the PECD recorded at these two photon energies, and in fact the peak value observed for $h\nu$ = 9.5 eV equates to a record chiral asymmetry ($= 2\left|b_1^{(\pm1)}\right|$) of ~37%. Previously, the largest PECD effect observed was a 32% forward-backward scattering asymmetry measured with epichlorohydrin enantiomers.[48]

In Fig. 8 we show the VMI PES and PECD measurements for (S)-(-)-β-pinene and S-(-)-sabinene which, in comparison to the above results, provide further contrasting behaviours. While the SPES and VMI-PES of β-pinene lack the clear vibrational structuring observed for limonene, 3-carene, and α-pinene, the PECD ($b_1^{(+1)}$) has quite distinct oscillations, whose depth is not dissimilar to that seen in 3-carene. Moreover, despite an overall shift between the PECD curves recorded at 9.0 eV and 9.5 eV photon energies, these modulations appear at common ionization energies, suggesting that they are indicative of some hidden structure underpinning the rather broad photoelectron band envelope. Given the well separated HOMO orbital and single conformation expected for β-pinene it is natural to suspect that this may be vibrational structure. The spacing of ~0.16 eV (≡1290 cm^{-1}) is very similar to the vibrational structures in α-pinene and limonene, and that was readily assignable as a stretching vibration of the C=C double bond from which the electron is ionized in those molecules. A similar interpretation seems plausible for β-pinene; ionization of the π HOMO can be expected to induce vibration around the exo-cyclic C=C double bond, and while the cation calculations do not indicate a highly localised C=C stretching normal mode, several normal modes (#37–#39) with frequencies around 1300 cm^{-1} do correspond to large amplitude nuclear displacements at the double bond location.

The sabinene PECD has been extracted from recordings made with the natural sabinene extract sample, after effective subtraction of the β-pinene contribution, and correction for the enantiomeric excess determined by GC[2] analysis. Full details of this data processing are provided in Supplementary Information. The results for sabinene PECD (Fig. 8) like the other isomers shown here, shows non-monotonic variations across the photoelectron band, at both photon energies studied.

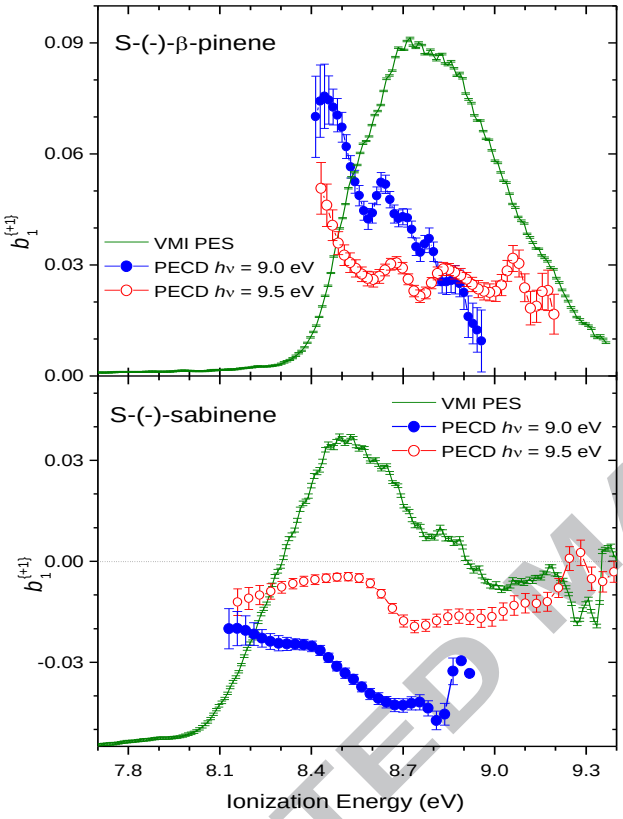

Figure 8

Discussion

There are features common to the four new $C_{10}H_{16}$ isomers (α-pinene, β-pinene, 3-carene, and sabinene) whose HOMO ionization we consider here. Their rigid bicyclic structure means that, unlike limonene, they effectively exist at room temperature and below as single conformers, and possess a single carbon-carbon double bond. The first ionization is that of the π orbital localised on this C=C bond and this HOMO is well separated from other orbitals. In the monocyclic limonene isomer the next orbital (HOMO-1) localized on the second C=C bond in the isopropenyl tail has a similar ionization energy to the HOMO, and the first band of the limonene photoelectron spectrum contains overlapping contributions from these two π orbitals.

There is also a clear qualitative divide between the character of the first photoelectron bands in these isomers: α-pinene and 3-carene, like limonene, have pronounced vibrational structures which are readily deduced to reflect excitation of the C=C stretching mode vibration in the cation following removal of the π electron localised at these bonds; neither β-pinene nor sabinene display such marked structure in their photoelectron spectra. In seeking a reason for these differences, we make the parallel observation that in the group displaying vibrationally structured spectra the ionized π orbital is endo-cyclic (internal to the six membered ring), whereas for two relatively unstructured

spectra the π orbital is exo-cyclic. Although providing poor results for β-pinene and sabinene, the FC simulations for these isomers suggest that with exo-cyclic double bonds, neither the HOMO nor the resulting vibrational motions are so well localised at the C=C position. An additional factor influencing the β-pinene and sabinene results is the ring opening of the strained ring in the cationic state predicted by some computational methods.[38,42] The large geometry changes pose a challenge for FC simulations and seem to preclude effective simulation. This is an issue that deserves further theoretical consideration.

Despite their having relatively featureless photoelectron bands, both β-pinene and sabinene do, however, show evidence of some modulation of their PECD, with relative spacings not dissimilar to those in seen in the other molecules' photoelectron spectra, and attributed to the C=C stretching motions. We should remark that PECD can provide more sensitive indications of underlying structure than the simple measurement of intensities in a photoelectron spectrum.[49] In the case of overlapping orbital ionizations the cross-sections leading to adjacent ion states may be rather similar, so hard to differentiate. PECD, on the other hand, may take very different values — even signs — for adjacent orbitals, helping reveal a hidden transition between ionization from one orbital to another with increasing energy. In the case of vibrations, to which it is increasingly obvious PECD also displays great sensitivity, more recent studies of chiral oxiranes have shown that dramatic switches in the $b_1^{(+1)}$ parameters can accompany weak vibrational excitations that are barely discernible in the photoelectron intensity (cross-section) curves.[22,23]

The strong influence of vibrational motion on the observed chiral asymmetry has been reported in both single-[20] and multi-photon[18,19] PECD investigations of limonene, so that similar observations here showing correlated PECD oscillations for 3-carene and α-pinene are unsurprising. It is further apparent that, in both these instances and also β-pinene, there is a steep decline in magnitude of the underlying PECD on passing from the low to high binding energy side of the HOMO band. In many previous studies with unresolved vibrational structure the PECD measurements have been seen to be rather constant across the photoelectron band, or at least rather slowly varying. Even without the resolved vibrational detail these terpene results are, therefore, somewhat unusual.

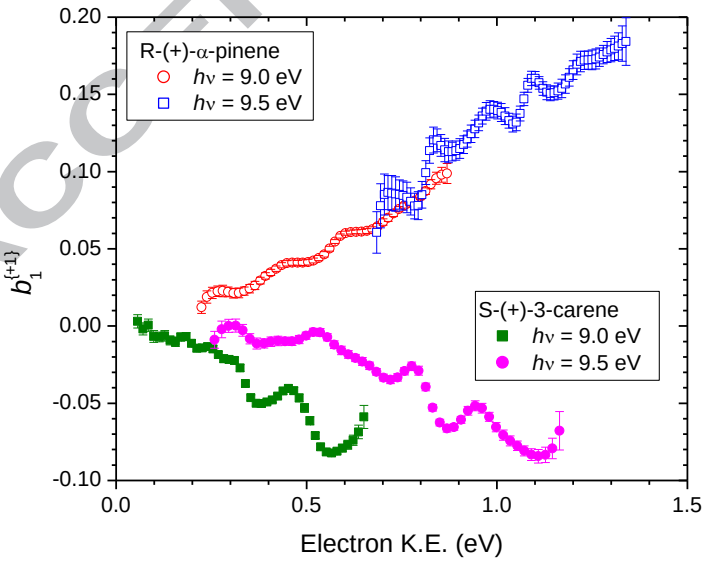

Figure 9

Other noteworthy features with α-pinene results are the record PECD magnitude (up to 37% asymmetry at low binding energy) and, for this specific molecule, the far bigger displacement between the PECD curves for the two photon energies studied here. In Fig. 9 we plot the α-pinene $b_1^{(+1)}$ values as a function of electron kinetic energy (rather than ionization energy as in Fig. 7). Now it can be seen that for this isomer there is an underlying trend for $b_1^{(+1)}$ to vary continuously and essentially monotonically from threshold to the highest electron kinetic energy observed, 1.5 eV. This trend reveals that for α-pinene the PECD is predominantly a function of electron kinetic energy alone, albeit over a relatively small energy range, and contrasts with the PECD behaviour of the other isomers. For example, the same plotting of the 3-carene PECD is shown in Fig. 9 with a very dissimilar appearance, which we can infer is indicative of some additional vibronic influence on the PECD.

Finally, it is worth noting that the photoelectron spectra provide a basis for clearly distinguishing several of these isomers by photoionization, given the different ionization onsets and vibrational envelopes. More generally, this approach to distinguishing isomeric form by threshold photoelectron spectroscopy is proving a powerful tool in VUV synchrotron studies of combustion etc. [50,51] In all cases here, including those particular pairings with less readily distinguishable photoelectron spectra (limonene/3-carene, β-pinene/sabinene) PECD appears as a very sensitive probe of chiral isomers, showing totally different behaviour for the five isomers considered here. Such a strong sensitivity of the $b_1^{(p)}$ observable to isomeric molecular structures has already been observed in the comparison of camphor to fenchone,[12,52] and is confirmed here. Naturally the PECD measurement also provides a clear means for distinguishing R and S enantiomers.

Summary

We have recorded PECD measurements for four bicyclic $C_{10}H_{16}$ terpene isomers under standardised conditions at photon energies of 9.0 eV and 9.5 eV, and augmented these with new measurements for the cyclic terpene limonene under the same conditions. In all cases, the outermost electron ionized is a π orbital located at a C=C double bond. The overall magnitude of the chiral asymmetry measured in PECD varies quite considerably between these isomers, from a few % (limonene) up to a record breaking 37% for α-pinene. For each molecule slow photoelectron spectra have also been obtained, and for those with an endo-cyclic double bond (limonene, α-pinene, 3-carene) these spectra display strong vibrational structure which we can largely attribute, using Franck-Condon simulations, to excitation of the C=C stretch in the ionized state. For β-pinene and sabinene there are, however, suggestions that the ionization induces a ring opening with consequences for the vibrational structure that need further investigation.

A particular point of interest is whether the PECD shows any vibrational influence, following the previously unexpected detection of this in small 3-membered ring oxiranes.[22,23] This was recently established also to be the case in the much larger cyclic terpene, limonene.[20] Such a phenomenon is now evident in 3-carene, α-pinene, and seemingly (despite the lack of strong vibrational structure in the SPES) is true also for β-pinene and possibly even sabinene. For 3-carene and the pinenes there is also evident an underlying trend for the PECD to show steep variation from high- to low-binding energy sides of the photoelectron band, and this is also quite unprecedented.

There is a clear need for further investigation, and here the advantage of these bicyclic terpene systems is that they exist as single conformers with well separated HOMO electrons. More pragmatically the reference data obtained here for molecules that are major constituents of many

natural products should facilitate the development of new approaches for the measurement of enantiomeric excess in vapours of volatile terpenes.

Acknowledgements

We should like to thank Cornelia Meinert, Iuliia Myrgorodska and Uwe Meierhenrich for the measurements by GC×GC of the chemical and enantiomeric purity of our samples.

This research has been supported (HG,RH) by the EU H2020 MSCA ITN “Aspire”.

We acknowledge the provision of beamtime by Synchrotron Soleil (beamtime Proposals No. 20151368, 20161224) and we thank the technical staff at Soleil for their support and for the smooth operation of the facility.

We are grateful for access to the University of Nottingham High Performance Computing Facility in support of the computational effort.

References

1 C. M. Wang, B. Barratt, N. Carslaw, A. Doutsi, R. E. Dunmore, M. W. Ward, and A. C. Lewis, Environ. Sci.-Process Impacts **19**, 528 (2017).

2 F. Klein, N. J. Farren, C. Bozzetti, K. R. Daellenbach, D. Kilic, N. K. Kumar, S. M. Pieber, J. G. Slowik, R. N. Tuthill, J. F. Hamilton, U. Baltensperger, A. S. H. Prevot, and I. El Haddad, Scientific Reports **6**, 36623 (2016).

3 http://www.leffingwell.com/chirality/chirality.htm, 2018

4 N. Yassaa and J. Williams, J. Chromatogr. A **1141**, 138 (2007).

5 G. Eerdekens, N. Yassaa, V. Sinha, P. P. Aalto, H. Aufmhoff, F. Arnold, V. Fiedler, M. Kulmala, and J. Williams, Atmos. Chem. Phys. **9**, 8331 (2009).

6 W. Song, M. Staudt, I. Bourgeois, and J. Williams, Biogeosciences **11**, 1435 (2014).

7 N. Yassaa, I. Peeken, E. Zollner, K. Bluhm, S. Arnold, D. Spracklen, and J. Williams, Environ. Chem. **5**, 391 (2008).

8 P. Q. Tranchida, I. Bonaccorsi, P. Dugo, L. Mondello, and G. Dugo, Flavour and Fragrance Journal **27**, 98 (2012).

9 I. Bonaccorsi, D. Sciarrone, A. Cotroneo, L. Mondello, P. Dugo, and G. Dugo, Rev. Bras. Farmacogn.-Braz. J. Pharmacogn. **21**, 841 (2011).

10 Y. Zhu, C. Y. Shao, H. P. Lv, Y. Zhang, W. D. Dai, L. Guo, J. F. Tan, Q. H. Peng, and Z. Lin, J. Chromatogr. A **1490**, 177 (2017).

11 M. M. Rafiee Fanood, N. B. Ram, C. S. Lehmann, I. Powis, and M. H. M. Janssen, Nat. Commun. **6**, 7511 (2015).

12 L. Nahon, L. Nag, G. A. Garcia, I. Myrgorodska, U. Meierhenrich, S. Beaulieu, V. Wanie, V. Blanchet, R. Géneaux, and I. Powis, Phys. Chem. Chem. Phys. **18**, 12696 (2016).

13 A. Kastner, C. Lux, T. Ring, S. Zullighoven, C. Sarpe, A. Senftleben, and T. Baumert, ChemPhysChem **17**, 1119 (2016).

14 J. Miles, D. Fernandes, A. Young, C. M. M. Bond, S. W. Crane, O. Ghafur, D. Townsend, J. Sá, and J. B. Greenwood, Analytica Chimica Acta **984**, 134 (2017).

15 L. Nahon, G. A. Garcia, and I. Powis, J. Elec. Spec. Rel. Phen. **204**, 322 (2015).

16 M. H. M. Janssen and I. Powis, Phys. Chem. Chem. Phys. **16**, 856 (2014).

17 M. M. Rafiee Fanood, M. H. M. Janssen, and I. Powis, Phys. Chem. Chem. Phys. **17**, 8614 (2015).

18 M. M. Rafiee Fanood, M. H. M. Janssen, and I. Powis, J. Chem. Phys. **145**, 124320 (2016).

19 S. Beaulieu, A. Ferre, R. Geneaux, R. Canonge, D. Descamps, B. Fabre, N. Fedorov, F. Legare, S. Petit, T. Ruchon, V. Blanchet, Y. Mairesse, and B. Pons, New J. Phys. **18**, 102002 (2016).

20 M. M. Rafiee Fanood, H. Ganjitabar, G. A. Garcia, L. Nahon, S. Turchini, and I. Powis, ChemPhysChem **19**, 921 (2018).

21 I. Powis, J. Chem. Phys. **140**, 111103 (2014).

22 G. A. Garcia, H. Dossmann, L. Nahon, S. Daly, and I. Powis, ChemPhysChem **18**, 500 (2017).

23 G. A. Garcia, L. Nahon, S. Daly, and I. Powis, Nat. Commun. **4**, 2132 (2013).

24 Y. Y. Li and F. Qi, Accts. Chem. Res. **43**, 68 (2010).

25 G. A. Garcia, B. K. C. de Miranda, M. Tia, S. Daly, and L. Nahon, Rev. Sci. Inst. **84**, 053112 (2013).

26 X. F. Tang, G. A. Garcia, J. F. Gil, and L. Nahon, Rev. Sci. Inst. **86**, 123108 (2015).

27 L. Nahon, N. d. Oliveira, G. Garcia, J. F. Gil, B. Pilette, O. Marcouille, B. Lagarde, and F. Polack, J. Synchrot. Radiat. **19**, 508 (2012).

28 G. A. Garcia, B. Gans, J. Kruger, F. Holzmeier, A. Roder, A. Lopes, C. Fittschen, C. Alcaraz, and J. C. Loison, Phys. Chem. Chem. Phys. **20**, 8707 (2018).

[29] J. C. Poully, J. P. Schermann, N. Nieuwjaer, F. Lecomte, G. Gregoire, C. Desfrancois, G. A. Garcia, L. Nahon, D. Nandi, L. Poisson, and M. Hochlaf, Phys. Chem. Chem. Phys. **12**, 3566 (2010).

[30] B. Mercier, M. Compin, C. Prevost, G. Bellec, R. Thissen, O. Dutuit, and L. Nahon, J. Vac. Sci. Tech. A **18**, 2533 (2000).

[31] M. Tia, B. Cunha de Miranda, S. Daly, F. Gaie-Levrel, G. A. Garcia, L. Nahon, and I. Powis, J. Phys. Chem. A **118**, 2765 (2014).

[32] L. Nahon, G. A. Garcia, C. J. Harding, E. A. Mikajlo, and I. Powis, J. Chem. Phys. **125**, 114309 (2006).

[33] M. J. Frisch, G. W. Trucks, H. B. Schlegel, G. E. Scuseria, M. A. Robb, J. R. Cheeseman, G. Scalmani, V. Barone, B. Mennucci, G. A. Petersson, H. Nakatsuji, M. Caricato, X. Li, H. P. Hratchian, A. F. Izmaylov, J. Bloino, G. Zheng, J. L. Sonnenberg, M. Hada, M. Ehara, K. Toyota, R. Fukuda, J. Hasegawa, M. Ishida, T. Nakajima, Y. Honda, O. Kitao, H. Nakai, T. Vreven, J. J. A. Montgomery, J. E. Peralta, F. Ogliaro, M. Bearpark, J. J. Heyd, E. Brothers, K. N. Kudin, V. N. Staroverov, T. Keith, R. Kobayashi, J. Normand, K. Raghavachari, A. Rendell, J. C. Burant, S. S. Iyengar, J. Tomasi, M. Cossi, N. Rega, J. M. Millam, M. Klene, J. E. Knox, J. B. Cross, V. Bakken, C. Adamo, J. Jaramillo, R. Gomperts, R. E. Stratmann, O. Yazyev, A. J. Austin, R. Cammi, C. Pomelli, J. W. Ochterski, R. L. Martin, K. Morokuma, V. G. Zakrzewski, G. A. Voth, P. Salvador, J. J. Dannenberg, S. Dapprich, A. D. Daniels, O. Farkas, J. B. Foresman, J. V. Ortiz, J. Cioslowski, and D. J. Fox, Gaussian 09 Revision D.01 (Gaussian Inc., Wallingford, CT, 2013).

[34] I. Pugliesi and K. Muller-Dethlefs, J. Phys. Chem. A **110**, 4657 (2006).

[35] M. A. Smialek, M. J. Hubin-Franskin, J. Delwiche, D. Duflot, N. J. Mason, S. Vronning-Hoffmann, G. G. B. de Souza, A. M. F. Rodrigues, F. N. Rodrigues, and P. Limao-Vieira, Phys. Chem. Chem. Phys. **14**, 2056 (2012).

[36] E. M. Neeman, J. R. A. Moreno, and T. R. Huet, The Journal of Chemical Physics **147**, 214305 (2017).

[37] I. Novak and B. Kovac, Spectrochimica Acta Part A-Molecular and Biomolecular Spectroscopy **61**, 277 (2005).

[38] D. Kubala, E. A. Drage, A. M. E. Al-Faydhi, J. Kocisek, P. Papp, V. Matejcik, P. Mach, J. Urban, P. Limao-Vieira, S. V. Hoffmann, S. Matejcik, and N. J. Mason, Int. J. Mass. Spec. **280**, 169 (2009).

[39] P. Lahiri, K. B. Wiberg, and P. H. Vaccaro, J. Phys. Chem. A **116**, 9516 (2012).

[40] V. A. Chuico, E. N. Manukov, Y. V. Chizhov, and M. M. Timoshenko, Khimiya Prir. Soedin., 639 (1985).

[41] T. Muller, K. B. Wiberg, and P. H. Vaccaro, J. Phys. Chem. A **104**, 5959 (2000).

[42] M. Q. Cao, J. Chen, W. Z. Fang, Y. Q. Li, S. L. Ge, X. B. Shan, F. Y. Liu, Y. J. Zhao, Z. Y. Wang, and L. S. Sheng, Eur. J. Mass Spectrom. **20**, 419 (2014).

[43] K. B. Wiberg, Y. G. Wang, M. J. Murphy, and P. H. Vaccaro, J. Phys. Chem. A **108**, 5559 (2004).

[44] Z. Kisiel and A. C. Legon, J. Am. Chem. Soc. **100**, 8166 (1978).

[45] S. Turchini, Journal of Physics: Condensed Matter **29**, 503001 (2017).

[46] G. A. Garcia, L. Nahon, C. J. Harding, and I. Powis, Phys. Chem. Chem. Phys. **10**, 1628 (2008).

[47] C. J. Harding and I. Powis, J. Chem. Phys. **125**, 234306 (2006).

[48] S. Daly, I. Powis, G. A. Garcia, H. Soldi-Lose, and L. Nahon, J. Chem. Phys. **134**, 064306 (2011).

[49] G. A. Garcia, H. Soldi-Lose, L. Nahon, and I. Powis, J. Phys. Chem. A **114**, 847 (2010).

[50] A. Bodi, P. Hemberger, D. L. Osborn, and B. Sztaray, J. Phys. Chem. Lett. **4**, 2948 (2013).

[51] J. Kruger, G. A. Garcia, D. Felsmann, K. Moshammer, A. Lackner, A. Brockhinke, L. Nahon, and K. Kohse-Hoinghaus, Phys. Chem. Chem. Phys. **16**, 22791 (2014).

[52] C. Lux, M. Wollenhaupt, T. Bolze, Q. Q. Liang, J. Kohler, C. Sarpe, and T. Baumert, Angew. Chem.-Int. Edit. **51**, 5001 (2012).

Figure Captions

Figure 1 The $C_{10}H_{16}$ terpenes discussed in this study, indicating specific enantiomers used for photoelectron circular dichroism measurements.

Figure 2 The first SPES band of limonene (Ref [20]) including a Franck-Condon simulation of the HOMO ionization vibrational profile. The inset shows adjacent photoelectron bands and the position of calculated vertical ionizations energies for these orbitals.

Figure 3 The first SPES band of α-pinene, including a Franck-Condon simulation of the vibrational profile of the band. The inset shows adjacent photoelectron bands below 10.5 eV with the position of calculated vertical ionizations energies for the HOMO and adjacent orbitals marked.

Figure 4 The first SPES band of 3-carene. Other detail as Fig. 3.

Figure 5 The first SPES band of β-pinene. Other detail as Fig. 3

Figure 6 The first SPES band of sabinene, corrected from the spectrum of natural 75% sabinene extract.

Figure 7 Parent mass-tagged (m/z 136) VMI PES and PECD measurements for R-(+)-limonene, S-(+)-3-carene, and R-(+)-α-pinene recorded under standardised conditions (see text). The VMI-PES has arbitrarily scaled intensity, but is plotted on the same ionization energy axis as the PECD measurements. These latter are shown as the chiral $b_1^{(+1)}$ parameter for the given enantiomer, extracted from a pair of images recorded with left- and right- circularly polarised radiation. The error bars are obtained by propagation of the Poisson counting statistics. Display of $b_1^{(+1)}$ parameters is supressed in regions where low photoelectron count rate (intensity) causes poor statistical quality (i.e. at the PES band fringes).

Figure 8 Parent mass-tagged (m/z 136) VMI PES and PECD for S-(-)-β-pinene and S-(-)-sabinene. The β-pinene PECD has been scaled to correct for the reduced e.e. (94%) of this sample. The sabinene data was corrected for impurities in the natural extract as described in Supplementary Information. Other detail as Fig. 7.

Figure 9 The PECD of R-(+)-α-pinene recorded at photon energies of 9.0 eV and 9.5 eV (fig. 7) as a function of electron kinetic energy. A similar plotting of the s-(+)-3-carene PECD data from Fig. 7 is also shown as a comparison.

Version 11 July 2018

Highlights

- PhotoElectron Spectroscopy & Circular Dichroism (PECD) with vibrational resolution
- α-pinene's PECD displays a record 37% chiral asymmetry factor
- Vibrational PECD effects parallel similar observations in cyclic limonene isomer
- Threshold electron spectra easily differentiate isomers (except sabinene/β-pinene)
- PECD would readily differentiate all pure isomers and their enantiomers